Field-Time Breakdown Characteristics of Air, N_2, CO_2, and SF_6

T. Liu, I. Timoshkin, *Senior Member, IEEE*, S. J. MacGregor, *Senior Member, IEEE*, M. P. Wilson, *Member, IEEE*, M. J. Given, *Senior Member, IEEE,* N. Bonifaci, *Senior Member, IEEE,* R. Hanna, *Member, IEEE*

***Abstract*—The dielectric performance of gases in insulation systems used in high voltage power and pulsed power applications is a subject of intensive theoretical and experimental investigation. Transient breakdown processes in gases stressed with short, high-field impulses, have been studied for many decades. However, there are still significant gaps in the understanding of the main breakdown processes and mechanisms associated with fast transient breakdown processes in gases. This knowledge is important for optimisation of gaseous insulating systems and for coordination of gaseous insulation in power and pulsed power apparatuses. This information is also required for the development of gas-filled components such as circuit breakers and plasma closing switches. The present work is aimed at analysis of the field-time breakdown characteristics of air, N_2, CO_2, and SF_6, using kinetic and drift-diffusion approaches. The kinetic approach is based upon the avalanche-to-streamer transition criterion, while the fluid drift-diffusion model requires self-consistent numerical solution of the continuity equations for charged species, and the Poisson equation for the electric field. The time to breakdown as a function of the applied field was obtained for all investigated gases. The obtained analytical results agree well with the experimental data reported in the literature, which suggests that both approaches can be used for insulation coordination, and for the development of gas-insulated power and pulsed power systems and components.**

***Index Terms*— Transient breakdown in gases, ionization front, time-field breakdown characteristics.**

I. Introduction

THE dielectric performance of gaseous insulation systems is a fundamental aspect that underpins the design and optimisation of gas-filled components and elements of high voltage power and pulsed power systems, [1]. Fast transient breakdown processes in different gases stressed with high electric fields have been extensively studied over many decades. A significant number of published papers focused on different experimental and modelling aspects of fast, μs and sub-μs, breakdown events in gases reflects the importance of understanding of complex fundamental breakdown processes. Development of plasma closing switches, [2], [3], circuit breakers, [4], and gas-insulated systems, [4], requires comprehensive information on such gas breakdown processes. Understanding of the basic breakdown mechanisms also provides a basis for further development of environmental, bio-medical and other practical applications of gas discharges, [5].

Computer modelling proved to be a useful and important approach to the analysis of fast breakdown processes in fluids. For example, in the late 1990s, the development of plasma streamers in air was studied by Morrow and Lowke, [6], by numerically solving the continuity equations for the charged species and the Poisson equation for the electric field. Later, in the early 2000s the transient breakdown mechanisms in gases were investigated by Sandia National Laboratories, [7]. However, despite significant research efforts in this field, the breakdown mechanisms and processes are still not fully understood. There is a lack of reliable engineering models for use in the optimisation of gas-filled power and pulsed power systems, and for coordination of gaseous insulation.

The present paper is aimed at the analysis and development of phenomenological equations for the ionization and electronic transport coefficients for different gases, to be used in analytical and computational approaches for modelling of the field-time breakdown characteristics of these gases with neutral gas density, N, in uniform electric field, E. Two models of gas breakdown, the fluid drift-diffusion model and kinetic model and were used in the present study, to predict formative breakdown times and breakdown fields for air, N_2, CO_2, and SF_6, - gases chosen due to their use in practical power, pulsed power, environmental and biomedical applications.

The kinetic breakdown model is based on the Meek "avalanche-to-streamer" transition (breakdown) criterion, and requires information on the electron transport characteristics in gases. The fluid drift-diffusion model is based on self-consistent numerical solution of the transport and continuity equations for ions and electrons, and the Poisson equation for the electric field. This model requires information on the ionization, attachment, and recombination coefficients of the gas, and the transport characteristics of different charged species, i.e. their mobilities and diffusion coefficients.

Both models used in the present investigation require

T. Liu, I. Timoshkin, S. J. MacGregor, M. P. Wilson, and M. J. Given are with the Department of Electronic and Electrical Engineering, University of Strathclyde, Glasgow, UK; N. Bonifaci, R. Hanna are with the G2E lab, CNRS, Grenoble, France (e-mail: ting.liu@strath.ac.uk; igor.timoshkin@strath.ac.uk; scott.macgregor@strath.ac.uk; mark.p.wilson@strath.ac.uk; m.given@strath.ac.uk; nelly.bonifaci@g2elab.grenoble-inp.fr; rachelle.hanna@g2elab.grenoble-inp.fr)

specific breakdown criteria in order to identify two main parameters, the breakdown field and time required for ionization to build up in the inter-electrode gap, culminating in breakdown, [8].

The breakdown kinetic model is based on the avalanche-to-streamer transition criterion. This criterion postulates that an electron avalanche propagating in a gas with an electron drift velocity, becomes unstable and transforms into a fast ionization front (streamer) when the total number of electrons in the avalanche head reaches ~10^8. According to [9], this build-up of ionization in the gap up to the critical avalanche size, followed by transition into a fast transient streamer mode, constitutes the breakdown event. Thus, the time required for ionization to build up in the inter-electrode gap is considered in the framework of the kinetic model as time to breakdown, $t_{br,}$. Typically, the total time to breakdown in gaseous breakdown processes is considered as a combination of two distinct time intervals, the statistical and formative times. The statistical time is interpreted as a time interval which is required for initial electron(s), capable of triggering of the avalanche ionization process, to appear in the inter-electrode gap. The statistical time has a stochastic nature and is difficult to predict for inclusion in analytical model(s). In the present paper, the total time to breakdown is considered as constituting the formative time only.

The breakdown criteria for the fluid drift-diffusion model is based on the establishment of an (almost) uniform distribution of the electron density across the gas-filled gap by a propagating ionization front.

In the models used in the present work, it is assumed that the initial electrons have appeared in the gap eliminating consideration of the statistical time. The ionization process in the gas-filled gap is therefore initiated immediately provided that the external electric field has sufficient magnitude. In the case of the computational fluid drift-diffusion model, a compact cluster of seed electrons is located close to the cathode. The time interval required for the ionization front to cross the inter-electrode gap at the field level that produces a uniform electron density behind this front is defined within the drift-diffusion model as "time to breakdown", t_{br}. This model was used to obtain both, time to breakdown, t_{br}, and reduced breakdown field, $(E/N)_{br}$, in a plane-plane electrode topology. The kinetic model was also used to obtain t_{br} for each investigated gas, over a wide range of values of $(E/N)_{br}$.

Both methods have their advantages and constraints. The kinetic approach provides a straightforward method of analysis of the breakdown behaviour of gases, if their ionization and transport parameters are known. The drift-diffusion model can be used for more detailed analysis of the breakdown processes. This model allows for investigation of the evolution of the ionization front in different electrode topologies, including topologies with highly-divergent electric fields and gas/solid interfaces. However, this approach requires the development of a computational code or use of specialist software (for example COMSOL) and computational resources, which may restrict the range of modelling parameters (time and field). Nevertheless, information extracted from both models can contribute to the coordination of gaseous insulation and the development of gas-filled components for high voltage power and pulsed power systems.

II. Fluid Drift-Diffusion Model

The fluid drift-diffusion approach is used in the present paper to describe the dynamic behaviour of three charged species during the development of ionization fronts in gases: electrons, negative ions, and positive ions. The time-dependent concentrations of these charged species are governed by the continuity equations, which link the rate of change of particle number in a specific volume with the divergence of the flux of these particles and their rates of generation, annihilation and diffusion. The charged particles move in the electric field which is governed by the Poisson equation, [10], [11]. Thus, using the continuity equations for the charged particles and the self-consistent electric field, propagation of the ionization front can be modelled.

A. Concentration of Charged Particles

The continuity equations for electrons, negative ions, and positive ions in the drift-diffusion approximation are the first-order partial differential equations given by (1) - (3). These equations can be solved, together with the Poisson equation (4), to describe the dynamics of the ionization front (streamer) in the gas.

$$\frac{\partial n_e}{\partial t} + \nabla \cdot \left(-n_e \mu_e \vec{E} - D\nabla n_e\right) = n_e\left(\alpha_{eff}\right)\left|\mu_e \vec{E}\right| - n_e n_p \beta \quad (1)$$

$$\frac{\partial n_p}{\partial t} + \nabla \cdot \left(n_p \mu_p \vec{E}\right) = n_e \alpha \left|\mu_p \vec{E}\right| - n_e n_p \beta - n_n n_p \beta \quad (2)$$

$$\frac{\partial n_n}{\partial t} + \nabla \cdot \left(-n_n \mu_n \vec{E}\right) = n_e \eta \left|\mu_n \vec{E}\right| - n_n n_p \beta \quad (3)$$

In (1) - (3), $\vec{E}$ is the electric field and t is time. The subscripts e, p, and n in these equations represent electrons, positive ions and negative ions respectively; the concentration and mobility of the charged particles are represented by n and μ respectively, with an index related to the specific species. β is the recombination rate coefficient, and D is the electron diffusion coefficient. When dealing with electronegative gasses, α_{eff} represents the effective ionization coefficient, which is the difference between the ionization coefficient α, and the attachment coefficient, η : $\alpha_{eff} = \alpha - \eta$.

For each gas the electronic diffusion coefficient is postulated to have a constant value or a weak dependency on electrical field in the range of E/N used the present study. The drift-diffusion approach is used to model the development of sub-μs ionisation fronts, thus ionic diffusion coefficients are not included in (1) - (3) as the diffusivity of ions is negligible as compared with the diffusivity of electrons. Also, due to the fast transient nature of the ionisation fronts, the recombination processes in the present model are approximated by using the same value of β for all electron-ion and ion-ion recombination events in each gas. Numerical values for all parameters, as used in the present study for all selected gases, are listed in Appendix I.

B. Electric Field

The generation and recombination of the charged particles during propagation of the ionization front into the bulk of the gas results in re-distribution of the electric field in the gap. Thus, the Poisson equation is used to describe the electric field which governs the development of the ionization front:

$$\nabla \cdot \vec{E} = e\left(n_p - n_n - n_e\right)\varepsilon^{-1} \quad (4)$$

where ε is the permittivity, and e is the elementary charge.

C. Ionization and Transport Parameters

The continuity equations (1) - (3) require detailed information on the ionization coefficients and on the transport parameters of the charged species. There is a significant number of published papers which provide the ionization, attachment (in the case of electronegative gases) and recombination coefficients of gases, and the transport characteristics of different charged species in gases, including their mobility, diffusion coefficients, and drift velocity. For example, the transport and swarm parameters of different gases as functions of the reduced field, the gas pressure, and the inter-electrode distance, are published in [12], [13]. The LXCAT database, [14], also provides an array of transport and swarm parameters for different gases.

However, there are different analytical function(s) reported in the literature for the ionization coefficients of the gases used in the present study. Some of these analytical functions known from the literature provide a good fit to the experimental data only within a limited range of field values. Thus, it is important to establish accurate analytical expressions, valid over a wide range of values of reduced applied field, (*E/N*), for the effective ionization coefficients of the gases used in the present study, which will allow for the use of these expressions in the fluid drift-diffusion and kinetic models.

Experimental values of the reduced effective ionization coefficient, α_{eff}/N, were obtained from the literature for all investigated gases. The fitting procedure in the OriginPro graphing software was then used to obtain analytical expressions for the function relating α_{eff}/N to the reduced electric field, *E/N*. Analysis of the literature data shows that no analytical functions are available for the ionization coefficients for all investigated gases, valid over the required range of values of *E/N*. Thus, for the successful use of both, fluid and kinetic, models, new analytical expressions for the effective ionization coefficients, valid over a wide range of values of *E/N*, needed to be developed. These are now presented and discussed.

1) Air

The experimental vales of α_{eff}/N for air, taken from [15], and [16], are shown in Figure 1 as functions of *E/N,* (squares and crosses). This figure also shows the analytical effective ionization curves proposed in [6], [7], [18], [19] and [20]. Values of E_s/N denote the transition between different fitting curves proposed in the literature for different field intervals for data sets [7] and [20]. This figure confirms that previously used analytical functions provide a reasonable fit to the experimental data only within limited ranges of the reduced field values.

In order to obtain an analytical curve which can be used for the whole range of *E/N* required for the present work, the experimental vales of α_{eff}/N, were fitted with function (5). Analytical curve (5), shown in Figure 1 as a solid line ("Present work") provides a good agreement with the experimental data, over a wide range of reduced electric fields, up to ~1500 Td.

$$\alpha_{eff}/N = 4\cdot10^{-20} exp\left(-985/\left(E/N+43\right)\right) - 30\cdot10^{-24}\ (\mathrm{m}^2) \quad (5)$$
$$94 < E/N < 1500\ (\mathrm{Td})$$

This fit also allow for the value for the critical field, $(E/N)_{cr}$ for air to be obtained. $(E/N)_{cr}$ is defined as the reduced field at which the effective ionization coefficient tends to zero, representing the value of reduced field below which an electron avalanche cannot develop. The critical field for air obtained in this work is ~94 Td; this value is close to the values of the critical field reported in [19], [21], and [22].

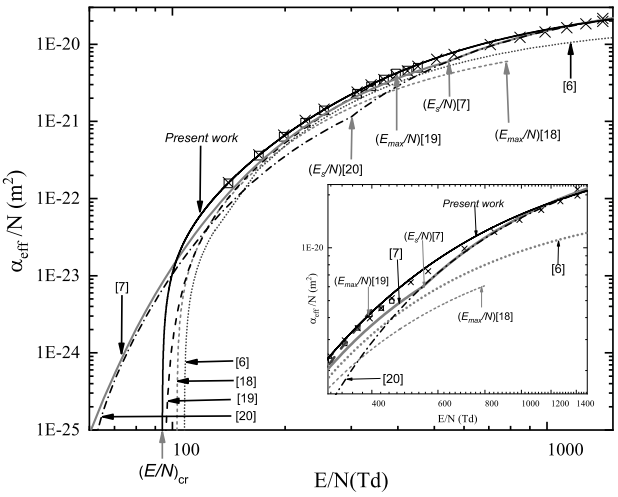

Fig. 1. α_{eff}/N as a function of *E/N* in air. Experimental data: □, [16]; × [15]. Fitting curves: dashed line, [19]; short dashed line, [18]; short dotted line, [6]; dashed - dotted line, [20]; solid gray line, [7]. Fitting curve: solid dark line, present work, (5). E_s/N represents the transition between different fitting curves from [7] and [20]; E_{max}/N represents maximum value of *E/N* for fitting curves [18] and [19].

2) Nitrogen

Being an electropositive gas, the attachment coefficient for N_2 is taken as $\eta = 0$, thus the concertation of negative ions in this gas is also zero, [59], [63], [64]. In Figure 2 experimental values of α/N for nitrogen from [23] and [24] are presented as open triangles and circles. Figure 2 also shows two analytical functions, taken from [7] and [25], however these functions do not provide values of α/N with a sufficient accuracy over the required range of values of *E/N*.

No single analytical function which would adequately fit the whole range of the reduced field (from ~60 Td to ~5000 Td) could be found for nitrogen. Therefore, the analytical fitting line obtained in the present work was constructed using (6) and (7), for two intervals of *E/N*, from 60 Td to 350 Td, and from 350 Td to 5000 Td.

$\alpha/N = 1.7\cdot10^{-20} exp\ (-800/(E/N-3))$ (m^2) (6)
$60 < E/N < 350$ (Td)

$\alpha/N = 3\cdot10^{-20} exp\ (-1000/(E/N))$ (m^2) (7)
$350 < E/N < 5000$ (Td)

These newly-obtained analytical fittings (6) and (7) will be used in the fluid drift-diffusion and kinetic models in the present paper. The critical field for nitrogen obtained using (6) is ~60 Td, which is in good agreement with the value reported in [26].

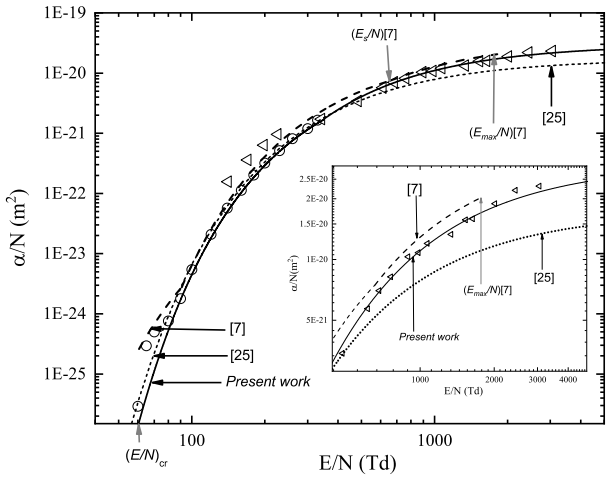

Fig. 2. α/N as a function of E/N in N_2. Experimental data: ◁, [23]; ○, [24]. Fitting curves: dashed line, [7]; dotted line, [25]; solid line, present work, (6)- (7). E_s/N represents the transition between different fitting curves from [7]; E_{max}/N represents the maximum field value for fitting curve [7].

3) Carbon Dioxide

Figure 3 shows the experimental α_{eff}/N data for CO_2 obtained in [24] as open points and crosses. This figure also includes the analytical curve for the effective ionization coefficient proposed in [27], which satisfies only a very limited range of E/N, ~1500 Td < E/N < ~3000 Td.

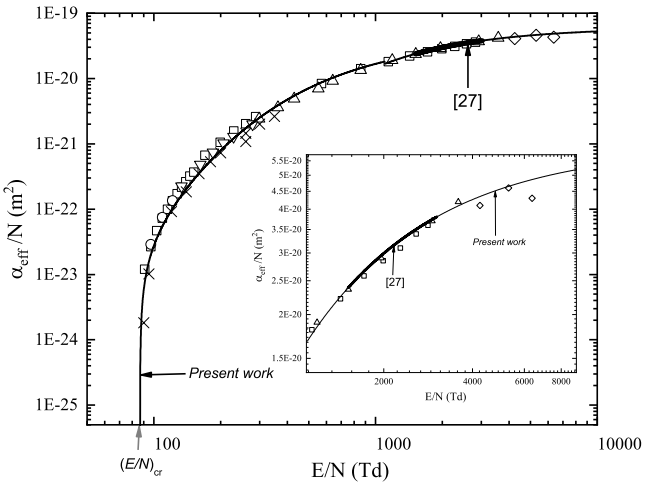

Fig. 3. α_{eff}/N as a function of E/N in CO_2. Experimental data points: × [24], □, ○, ▽, △ and ◇, [17]. Fitting curves: bold solid line, [27]; solid line, present work, (8)-(9).

As in the case of nitrogen, two analytical curves, (8) - (9), were obtained in the present work to provide a full analytical description of the effective ionization coefficient in the range from ~86 Td to ~10^4 Td. The obtained composite analytic curve ("Present work") is shown in Figure 3.

$\alpha_{eff}/N = 4.3\cdot10^{-20} exp\ (-986/\ (E/N+49)) - 30\cdot10^{-24}$ (m^2) (8)
$86 < E/N < 1100$ (Td)

$\alpha_{eff}/N = 6.07\cdot10^{-20} exp\ (-1414/\ (E/N))$ (m^2) (9)
$1100 < E/N < 10000$ (Td)

The critical field for CO_2, obtained using analytical fitting curve (8), is ~86 Td, which is close to the values of the critical field for CO_2 reported in [28] and [29].

4) Sulphur Hexafluoride

Figure 4 shows the experimental values of α_{eff}/N for SF_6 as open circles (data from [32]). The analytical ionization coefficient proposed in [30], and shown in this figure as a dashed line, demonstrates a noticeable deviation from the experimental values for high values of E/N, above ~2500 Td, and for the values of E/N in the range of 400 - 500 Td.

Analytical fitting line for α_{eff}/N was obtained for SF_6 in the present work in the range from ~360 Td to ~5000 Td. This line is given by (10) and shown in Figure 4.

$\alpha_{eff}/N = -9.06\cdot10^{-20} exp\ (-(E/N)/2875) + 8\cdot10^{-20}$ (m^2) (10)
$360 < E/N < 5000$ (Td)

Fitting curve (10) provides a good match to the experimental data over the full range of values of E/N, from 360 Td to 5000 Td. Fitting curve (10) also provides a critical field value of ~360 Td for SF_6, which is in good agreement with the values previously reported in [31], [32] and [33].

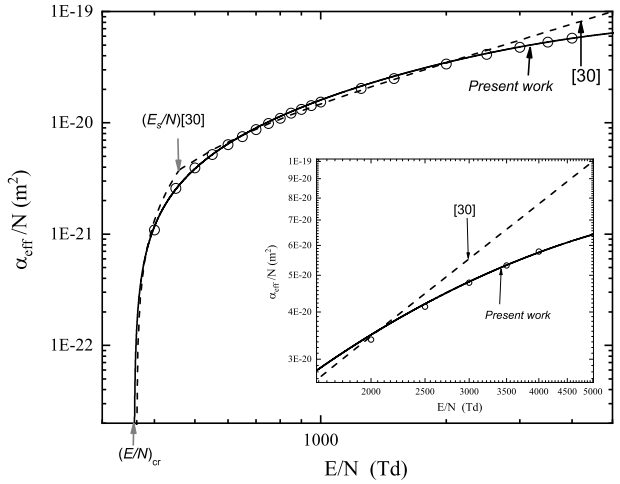

Fig. 4. α_{eff}/N as a function of E/N in SF_6. Experimental data: ○ [32]. Fitting curves: dashed line, [30]; solid line, present work, (10). E_s/N represents the transition between different fitting curves from [30].

Table I shows the values of $(E/N)_{cr}$ obtained in the present paper, and the values of $(E/N)_{cr}$ available in the literature for the same gases. There is good agreement between the $(E/N)_{cr}$ values obtained for air, N_2, CO_2 and SF_6 in the present paper

and previously reported values.

TABLE I
CRITICAL FIELD FOR INVESTIGATED GASES

Gas	$(E/N)_{cr}$,(Td) from present work	$(E/N)_{cr}$,(Td) from literature
Air	94	94.7 [19] 99.4 [21] 98.5 [22]
N_2	60	<60 [26]
CO_2	86	86 [28] 82 [29]
SF_6	360	359 [34] 360 [31], [32], [33] 361[35] 362 [36], [37]

D. Secondary Electron Emission Process

The Townsend discharge model postulates that the development of a self-sustained electron avalanche is supported by secondary electron emission, which is described by Townsend's secondary ionization coefficient, γ. This coefficient is defined as the number of electrons generated by a single positive ion colliding with the cathode. Typical values of γ are in the range from 10^{-2} to 10^{-4}.

However, there are other ionization processes that may affect the development of electron avalanches and streamers in gases. These processes include: photoionization, which is an important factor in the case of positive streamers, and background ionization. In the case of a negative ionization front in a gas at atmospheric pressure, the roles of photoionization and background radiation are inferior to the electron emission from the cathode, described by γ, [7], [38], and [39]. This has led to modelling approaches where the effects of photoionization and background radiation have been omitted. For example, photoionization was not taken into account in [40], where only the secondary electron emission process was included in the model. A similar approach was adopted in [41], where it was stated that background ionization has a negligible effect on the development of negative streamers. Background ionization was also excluded from the streamer model in atmospheric air in [42], [43], and [44]. These assumptions are also made by the authors of this paper, and only the process of emission of secondary electrons from the cathode, with $\gamma = 0.004$, was directly included in the fluid drift-diffusion model, (1) - (4). However, it can be considered that the role of background ionization has been taken into account, as a source for the seed population of electrons used in the fluid drift-diffusion model, and for the presence of an initiating electron for the formation of the avalanche in the kinetic model.

E. Mobility of Electrons

One of the important transport parameters required for both, drift-diffusion and kinetic models is electron mobility, μ_e. In Figure 5 the experimental values of the product of electron mobility and particle density, $\mu_e N$, are shown as open and closed symbols for: air, [45]; N_2, [46]; CO_2, [47]; and SF_6, [32]. The experimental vales of $\mu_e N$ were fitted with analytical curves (11) - (14) for each specific gas:

Air
$$\mu_e N = 3.361 \cdot 10^{24} (E/N)^{-0.222} \quad (\mathrm{m \cdot V \cdot s})^{-1} \tag{11}$$

Nitrogen
$$\mu_e N = 1.7 \cdot 10^{24} (E/N)^{-0.09} \quad (\mathrm{m \cdot V \cdot s})^{-1} \tag{12}$$

Carbon dioxide
$$\mu_e N = 8.68 \cdot 10^{24} (E/N)^{-0.416} \quad (\mathrm{m \cdot V \cdot s})^{-1} \tag{13}$$

Sulphur hexafluoride
$$\mu_e N = 3.085 \cdot 10^{24} (E/N)^{-0.284} \quad (\mathrm{m \cdot V \cdot s})^{-1} \tag{14}$$

Functions (11) - (14) are shown in Figure 5 as solid lines.

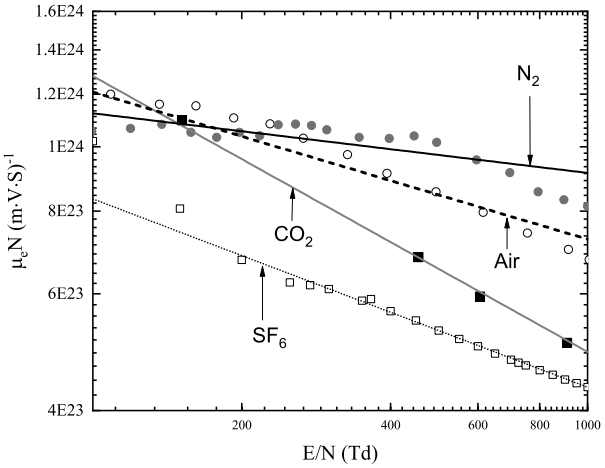

Fig. 5. $\mu_e N$ as a function of E/N. Simulation data from literature: ○ [45]. Experimental data from literature: ● [46], ■ [47], □ [32]. Fitting curves for present work: dashed line, air, (11); solid dark line, N_2, (12); solid gray line, CO_2, (13); dotted line, SF_6, (14).

III. FLUID DRIFT-DIFFUSION MODEL

A parallel-plane electrode topology was used in the present work to model the development of fast ionization fronts in gases. The ionization front model is based on continuity equations, (1) - (3), and Poisson's equation, (4). The model was implemented in COMSOL Multiphysics software, using a 2D geometry with symmetrical electrodes in the cylindrical coordinate system, with the z-axis directed vertically (r is the radial coordinate). The inter-electrode gap was set to 1.5 mm, the radius of both plane electrodes was 3 mm, and the gas pressure in all cases was set to 1 atm (absolute).

The top plane electrode (cathode) was energised with a negative potential, the lower electrode was kept at zero potential. A cluster of seed electrons, which simulates initial electrons produced by natural background radiation, was located at the centre of the cathode. The initial electron concentration, n_{e0}, followed a Gaussian distribution, [40]:

$$n_{e0} = n_0 exp\left(-\frac{(\mathrm{r}-r_0)^2}{2\sigma_r} - \frac{(\mathrm{z}-z_0)^2}{2\sigma_z}\right) \tag{15}$$

where n_0 is the maximum concentration of seed electrons, $n_0 = 10^{12}$ m^{-3}, [10]. The centre of the electron cluster was positioned at $r_0 = z_0 = 0$. The parameters controlling the change in the electron density along the r and z coordinates

were set to $\sigma_r = \sigma_z = 0.25$ mm, as proposed in [18].

IV. Breakdown Criterion

A. Fluid Drift-diffusion Model

The computational procedure to solve (1) - (4) starts at time t_0, when the magnitude of the applied negative voltage is set to a user-defined value, U_0. The electron density associated with the development of the ionization front (streamer) is then obtained after a time interval specified by the user, t_{br}. If the electron density was not distributed uniformly, the magnitude of the applied voltage was increased by ΔU, and the computational process was repeated. The voltage magnitude was increased in steps, ΔU, until the uniform distribution of the electron density in the z direction across the gap was observed. This marks the voltage condition, U_{br}, where the ionization front just reaches the opposite (ground) electrode in the time interval, t_{br}, which is recorded as time to breakdown. Convergence of the computational algorithm was achieved by the selection of the appropriate mesh size at each step of the computational process.

B. Kinetic Model

According to the Townsend model of an electron avalanche, the electronic charge in the avalanche head, Q, increases exponentially with propagation time, t:

$$Q \propto \exp(\nu t) \tag{16}$$

where ν is ionization frequency. Following the Meek criterion, the electron avalanche transforms into a streamer (streamer breakdown criterion) when the number of electrons in the avalanche head reaches ~10^8. Thus, the following condition can be obtained:

$$\nu t_{br} \geq 18 \tag{17}$$

The ionization frequency, ν, is the product of the effective ionization coefficient, α_{eff}, and the electron drift velocity, v_{drift}: $\nu = \alpha_{eff} v_{drift}$. The drift velocity itself is the product of electron mobility and the electric field: $v_{drift} = \mu_e E$. Thus, the relationship between time to breakdown, t_{br}, and reduced breakdown field, E/N, can be established:

$$t_{br} N = 18/[(\alpha_{eff}\mu_e)(E/N)] \tag{18}$$

where both, α_{eff} and μ_e, are functions of E/N. This kinetic relationship will be used in Section V to obtain field-time breakdown characteristics for gases.

V. Simulation Results

Computational modelling of the development of ionization fronts in air, N_2, CO_2, and SF_6, have been conducted using the fluid drift - diffusion model, (1) - (4). This model was used to obtain breakdown voltages, for values of time to breakdown covering a range of values of reduced field. The kinetic model has also been used to calculate breakdown times as a function of field, over a range of reduced field values for the gases investigated. The nominal average velocities of propagation of the ionization fronts have also been obtained from the fluid drift diffusion model. The ionization front propagation velocity, $\bar{v}_{front}$, is defined as the length of the inter-electrode gap, ℓ, divided by the time to breakdown, t_{br}, i.e. the time required for the ionization front to form, cross the gap and reach the anode:

$$\bar{v}_{front} = \ell / t_{br} \tag{19}$$

This definition of the nominal average streamer velocity was used in [48], [49], and [50].

A. Average Velocity of Ionization Front

The nominal average ionization front velocities in air, N_2, CO_2, and SF_6, obtained using (19), are shown in Figure 6 as functions of E/N. These results demonstrate that $\bar{v}_{front}$ increases with an increase in the applied electric field. For example, $\bar{v}_{front}$ in air at atmospheric pressure increases from ~$0.13 \cdot 10^6$ m/s at $4 \cdot 10^6$ V/m, up to ~$5.7 \cdot 10^6$ m/s at $115 \cdot 10^6$ V/m. These values are in the range of those reported in the literature: [18] indicates that the average velocity of streamers in air is $(0.1\text{-}10) \cdot 10^6$ m/s; while [50] and [51] provide the value of $2 \cdot 10^6$ m/s for this velocity.

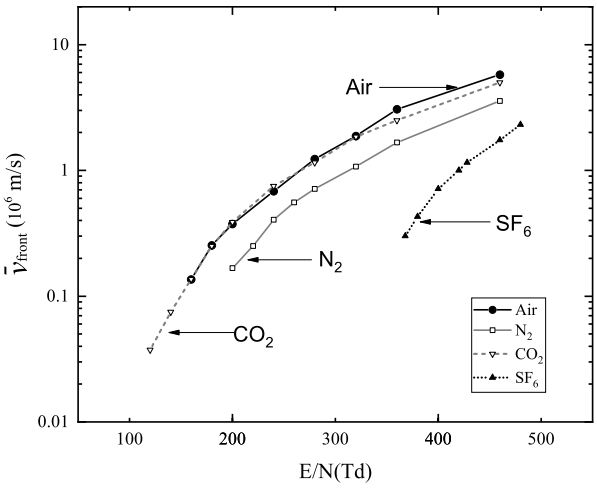

Fig. 6. Nominal average velocity of the ionization front, $\bar{v}_{front}$, as a function of E/N. ● Air; □ N_2; ▽ CO_2; ▲ SF_6. Connecting lines are given for visual guidance only.

As can be seen from Figure 6, $\bar{v}_{front}$ for CO_2 is similar to that for air, for all values of E/N, [52]. For N_2, $\bar{v}_{front}$ is lower than that for air and CO_2. This is confirmed by the published data, for example, [53] and [54] quote ~10^5 m/s and ~10^4 m/s as average streamer velocities in N_2. SF_6 has the lowest nominal average velocity, ~ $0.3 \cdot 10^6$ m/s, at ~368 Td as compared with the average velocities obtained for other investigated gases at ~360 Td.

B. Field-Time Characteristics

The breakdown parameters: time to breakdown multiplied by the particle density, Nt_{br}, and reduced breakdown field $(E/N)_{br}$, obtained via the fluid drift-diffusion model (1) – (4), and the kinetic model (18), have been plotted as time - field breakdown curves. Figures 7 – 10 show Nt_{br} as a function of $(E/N)_{br}$ for air, N_2, CO_2, and SF_6, together with the experimental breakdown data from [8]. The kinetic model provides the values of Nt_{br} (shown as solid lines) in a wide range of the reduced breakdown fields. However, due to computational limitation, the results obtained using the fluid drift-diffusion model (shown as solid dots) were restricted to values of $(E/N)_{br}$ less than 500 Td.

It can be seen that both, the computational fluid drift-diffusion model and the kinetic model provide a good agreement with the experimental breakdown characteristics available for air, N_2, and SF_6. No experimental field - time breakdown data for CO_2 was found in the literature.

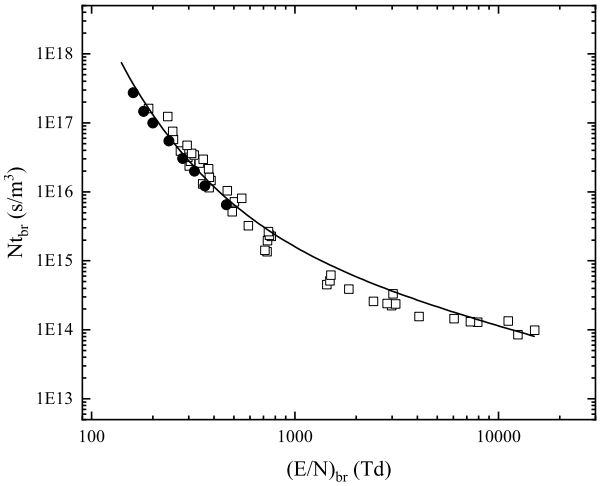

Fig. 7. Nt_{br} as a function of $(E/N)_{br}$ in air. □ experimental data, [8]; ● fluid drift-diffusion model, (1) - (4); — kinetic approach, (18).

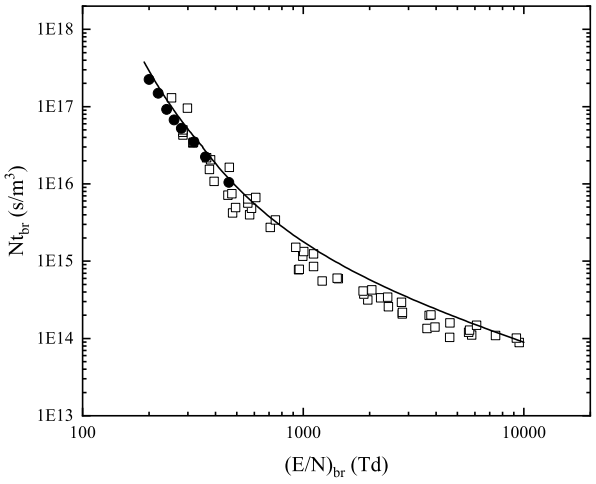

Fig. 8. Nt_{br} as a function of $(E/N)_{br}$ in N_2. □ experimental data, [8]; ● fluid drift-diffusion model (1)-(4); — kinetic approach (18).

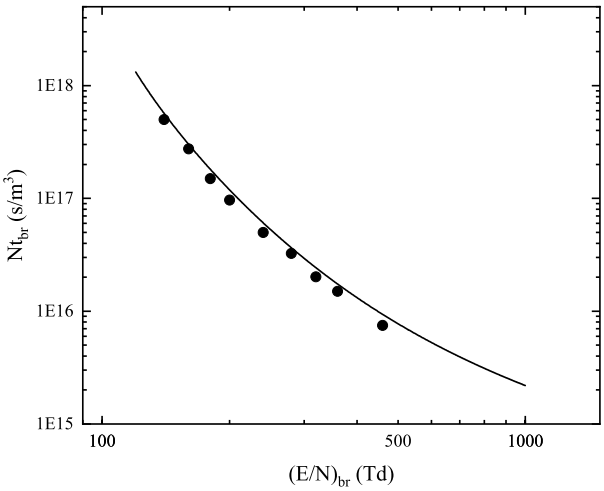

Fig. 9. Nt_{br} as a function of $(E/N)_{br}$ in CO_2. ● fluid drift-diffusion model (1) - (4); — kinetic approach (18).

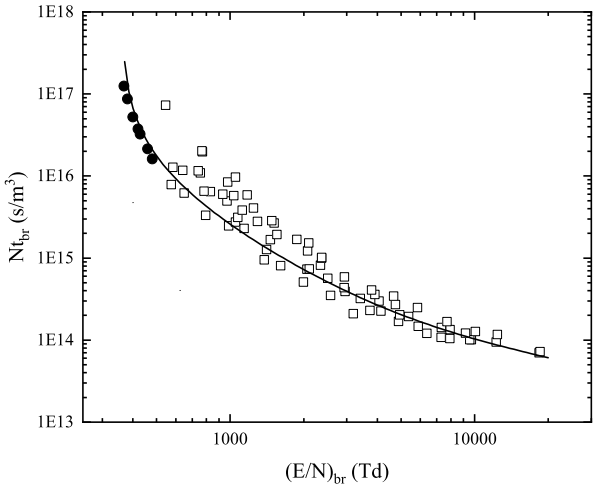

Fig.10. Nt_{br} as a function of $(E/N)_{br}$ in SF_6. □ experimental data, [8], ● fluid drift-diffusion model, (1) - (4); — kinetic approach ,(18).

Figure 11 summarises the results of kinetic modelling and shows Nt_{br} as a function of $(E/N)_{br}$ for all investigated gases, obtained using (18). This representation of $Nt_{br}(E/N)$ curves facilitates analysis of the time-breakdown field performance of the different gases. For lower fields, $(E/N)_{br}$ <1000 Td, SF_6 demonstrates significantly longer formative time (greater Nt_{br} values) as compared with other gases, and this difference increases as $(E/N)_{br}$ decreases. Air and CO_2 show almost identical breakdown performance for $(E/N)_{br}$ <1000 Td, N_2 demonstrates slightly higher values of Nt_{br} than air and CO_2, but lower than SF_6 in this range. It is interesting to note that, for field strengths above ~3000 Td, the time - breakdown field curve for air converges with that for SF_6, while the $Nt_{br}(E/N)$ curve for N_2 shows lower Nt_{br} values than those for SF_6 and air. These scaling relations can be used in analysis of the time required for the ionization front to cross the inter-electrode gap for different levels of applied field, and at different gas pressures.

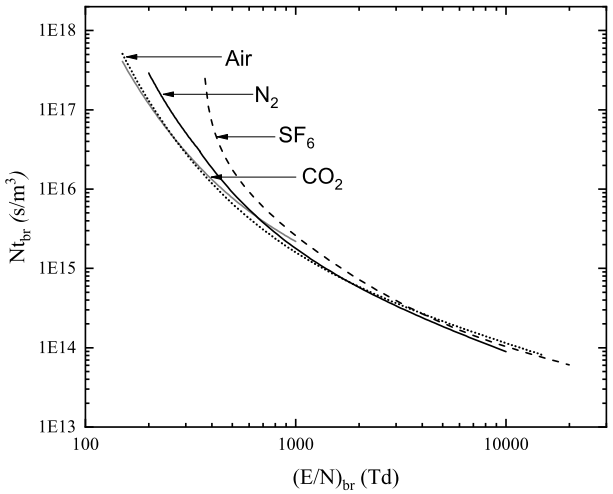

Fig.11. Nt_{br} as function of $(E/N)_{br}$, obtained by (18). Dotted line: air; solid dark line: N_2; solid gray line: CO_2; dashed line: SF_6.

Figure 12 shows the reduced breakdown field values for different values of Nt_{br}, for all investigated gases. It can be seen that at longer breakdown times (i.e. higher values of Nt_{br} at the constant pressure), SF_6 demonstrates higher values of breakdown field than the other gases. However, for lower values of Nt_{br}, all gases show similar reduced breakdown fields - for example, for $Nt_{br} = 3 \cdot 10^{15}$ (s/m^3), $(E/N)_{br}$ for all investigated gases is in the range of 700 - 1000 Td (although air and N_2 show lower values of $(E/N)_{br}$ than SF_6 and CO_2). With further decrease in Nt_{br}, CO_2 and SF_6 show similar values of $(E/N)_{br}$, as can also be seen in Figure 11.

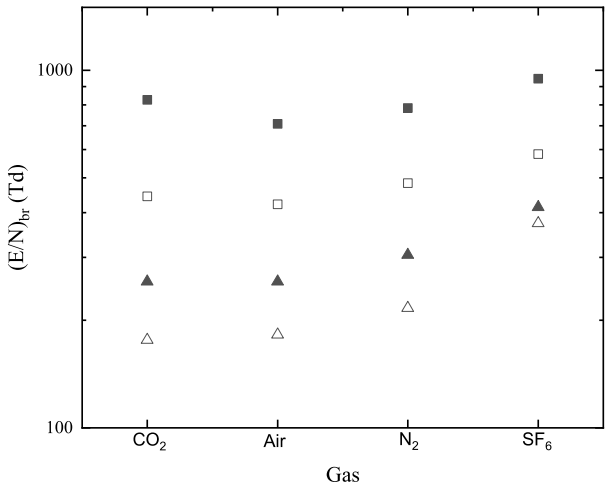

Fig.12. $(E/N)_{br}$ for investigated gases for specific values of Nt_{br}. △ $2 \cdot 10^{17}$ (s/m^3); ▲ $5 \cdot 10^{16}$ (s/m^3); □ $1 \cdot 10^{16}$ (s/m^3); ■ $3 \cdot 10^{15}$ (s/m^3).

VI. Conclusion

In the present work, two models that allow the simulation and prediction of the time - field breakdown characteristics were used to investigate breakdown behaviour of different gases. The first model is based on the fluid drift - diffusion computational approach, which can simulate the transient development of the ionization front in different gases. The second model is based on the kinetic approach to gas breakdown and uses the avalanche-to-streamer transition criterion. Both approaches were used for modelling of the field - time breakdown characteristics of air, N_2, CO_2, and SF_6 - gases, for which the ionization and transport parameters are known. Based on the literature data, the analytical equations for the effective ionization coefficients and for electronic mobility for these gases were obtained in a wide range of E/N used in the present study.

The analytical relationship between the time to breakdown (the time required for the ionization front to cross the gap) and the breakdown voltage (minimum voltage applied to the electrode system at which the ionization front can bridge the gap) were obtained for all gases considered in the present work. It was shown that the obtained analytical results demonstrate good agreement with the experimental field-time breakdown data published in [8], [9], and [55].

The results obtained in this work are presented as time-field breakdown characteristics: the product of the particle density and the time to breakdown, Nt_{br}, versus the reduced electric field, $(E/N)_{br}$. It is known that, within the framework of the gas kinetic approach, the mean free path of an electron is a function of the reciprocal of the gas particle density, $1/N$. In this approach, the energy required to ionise neutral atoms or molecules has no dependence on pressure (gas particle density). Thus, using dimensional analysis, it can be shown that, both, the applied electric field required for electrons to gain such energy, and the energy gaining frequency (the reciprocal of the time required for electrons to gain this energy, [27]), are functions of N, [69]. Therefore, the parameters Nt_{br} and $(E/N)_{br}$ can be used to establish scaling relations for gas discharges and breakdown in gases. Since these relations imply that the breakdown parameters are the same at fixed values of (E/N), they can be employed for analysis of the breakdown behaviour of gases in similar electrode topologies, at different pressures. The analytical time-field breakdown characteristics, Nt_{br} vs $(E/N)_{br}$, obtained in this work fit well the experimental results for air, N_2, and SF_6, obtained and presented in [8]. In the tests conducted in [8], the applied voltage was in the range from 5 kV to 30 kV (in the case of air), from 4 kV to 20 kV (in the case of N_2), and from 4 kV to 25 kV (in the case of SF_6), while the gas pressures used were between ~$1.3 \cdot 10^{-3}$ atm and ~1 atm. The maximum inter-electrode gap was 6 cm for all gases, while the minimum gaps were different: 0.13 mm for air and N_2, and 0.051 mm for SF_6. Analysing the experimental time-breakdown data presented in [8] for different inter-electrode gaps, it can be noted that the values of the pressure-distance product, $p \times d$, were in the range from several thousandths of one atm·cm, to ~ 0.1 atm·cm. These values of $p \times d$ correspond to the right-hand side of the Paschen curve for all investigated gases. Thus, the models developed in the presented paper and the obtained scaling relations can be stated to be valid for the experimental parameters used in [8]. Further experimental studies are required in order to establish the full range of operational parameters within which the proposed scaling relations are valid.

The proposed models will help in further investigation of the transient breakdown processes in gases, and can be used in the design and optimisation of gas-filled, high voltage sub-systems and components, for use in power and pulsed power systems.

APPENDIX I.

Appendix I presents the swarm parameters used in both, the fluid drift-diffusion model, (1) - (4), and the kinetic model, (18). The reduced effective ionization coefficient, $\alpha_{eff}/N = (\alpha - \eta)/N$ (m^2), is given as a function of reduced electric field, E/N (Td, 1 Td=10^{21} V·m^2), for different ranges of E/N, for all investigated gases. The gas pressure used in the calculation of all parameters in the present work was equal to 10^5 Pa, providing a corresponding value of the particle number density of $N = 2.5 \cdot 10^{25} (1/m^3)$ at room temperature. Tables II – V provide all ionization and transport coefficients used in the present paper.

TABLE II
SWARM PARAMETERS OF AIR IN PRESENT MODEL

Parameter	Value/function used in the present paper	References
$D(\frac{m^2}{s})$	0.18	[18], [56]
$\mu_p\ (\frac{m^2}{V \cdot s})$	$2.34 \cdot 10^{-4}$	[6], [57]
$\mu_n\ (\frac{m^2}{V \cdot s})$	$2.7 \cdot 10^{-4}$ $E/N > 50Td$ $1.86 \cdot 10^{-4}$ $E/N < 50Td$	[6], [57]
$\beta\ (\frac{m^3}{s})$	$2 \cdot 10^{-13}$	[6], [10], [58]

TABLE III
SWARM PARAMETERS FOR N_2 USED IN THE PRESENT MODEL

Parameter	Value/function used in the present paper	References
$D(\frac{m^2}{s})$	0.18	[59]
$\mu_p\ (\frac{m^2}{V \cdot s})$	$2.5 \cdot 10^{-4}$	[60], [61]
$\beta\ (\frac{m^3}{s})$	$\sim 1 \cdot 10^{-13}$	[62]

TABLE IV
SWARM PARAMETERS FOR CO_2 USED IN THE PRESENT MODEL

Parameter	Value/function used in the present paper	References
$D(\frac{m^2}{s})$	~ 0.1	[65]
$\mu_p\ (\frac{m^2}{V \cdot s})$	$6.52 \cdot 10^{-5} exp(-(E/N)/399) + (6.96 \cdot 10^{-5})$ $50 \le E/N \le 1200Td$	Data from [66]; Fitting equation from present work
$\mu_n\ (\frac{m^2}{V \cdot s})$	$6.47 \cdot 10^{-6} exp(((E/N) - 7.4)/86.7) + (1.22 \cdot 10^{-4})$ $5 \le E/N \le 150Td$	Data from [66]; Fitting equation from present work
$\beta\ (\frac{m^3}{s})$	$\sim 1 \cdot 10^{-13}$	[67]

TABLE V
SWARM PARAMETERS FOR SF_6 USED IN THE PRESENT MODEL

Parameter	Value/function used in the present paper	References
$D(\frac{m^2}{s})$	$3.553 \cdot 10^{-2} (E/N)^{0.2424}$ $E/N < 650Td$	[30]
$\mu_p\ (\frac{m^2}{V \cdot s})$	$6.0 \cdot 10^{-5}$ $E/N < 120Td$ $1.216 \cdot 10^{-5} \ln(E/N) + 0.01 \cdot 10^{-4}$ $120Td < E/N < 350Td$ $-1.897 \cdot 10^{-5} \ln(E/N) + 1.83 \cdot 10^{-4}$ $E/N > 335Td$	[30]
$\mu_n\ (\frac{m^2}{V \cdot s})$	$1.69 \cdot 10^{-10} (E/N)^2 + 0.53 \cdot 10^{-4}$ $E/N < 500Td$	[30]
$\beta\ (\frac{m^3}{s})$	$\sim 10 \cdot 10^{-13}$	[68]

REFERENCES

[1] J. Lehr, P. Ron, "Foundations of Pulsed Power Technology", *Wiley-IEEE Press*, 2017.

[2] G. Schaefer, M. Kristiansen, A. Guenther, "Gas Discharge Closing Switches", *Springer Science + Business Media*, 1990.

[3] A. R. Dick, S. J. MacGregor, M. T. Buttram, R. C. Pate, L. F. Rinehart, K. R. Prestwich, "Breakdown phenomena in ultra-fast plasma closing switches", *IEEE Transactions on Plasma Science*, vol. 28, no. 5, pp. 1456-1462, 2000.

[4] A. Haddad, D. F. Warne, "Advances in High Voltage Engineering", IET, 2004.

[5] M. Laroussi, M. G. Kong, G. Morfill, W. Stolz, "Plasma Medicine: Applications of Low-Temperature Gas Plasmas in Medicine and Biology", *Cambridge University Press*, 2012.

[6] R. Morrow, J. J. Lowke, "Streamer propagation in air", *J. Phys. D: Appl. Phys.*, vol. 30, pp. 614-627, 1997.

[7] L. K. Warne, R. E. Jorgenson, S. D. Nicolaysen, "Ionization coefficient approach to modeling breakdown in nonuniform geometries", SANDIA Report No. SAND2003-4078, 2003.

[8] P. Felsenthal, J. M. Proud, "Nanosecond-Pulse Breakdown in Gases", *Phys. Rev.*, vol. 139, no. 6A, pp. A1796–A1804, 1965.

[9] R. C. Fletcher, "Impulse breakdown in the 10^{-9} sec range of air at atmospheric pressure", *Phys. Rev.*, vol. 76, no. 10, pp. 1501-1511, 1949.

[10] G. E. Georghiou, A. P. Papadakis, R. Morrow, A. C. Metaxas, "Numerical modelling of atmospheric pressure gas discharges leading to plasma production", *J. Phys. D Appl. Phys.*, vol. 38, no. 20, pp. R303-R328, 2005.

[11] C. Li, W. J. M. Brok, U. Ebert, "Deviations from the Local Field Approximation in Negative Streamer Heads", *J. Appl. Phys.*, vol. 101, no. 12, pp. 123305 1–14, 2007.

[12] J. Dutton, "A survey of electron swarm data", *J. Phys. Chem. Ref. Data*, vol. 4, pp.577-856, 1975.

[13] J. W. Gallagher, E. C. Beaty, J. Dutton, and L. C. Pitchford, "An annotated compilation and appraisal of electron swarm data in electronegative gases", *J. Phys. Chem. Ref. Data*, vol. 12, no. 1, pp.109-152. 1983.

[14] [online] Available: www.lxcat.net, retrieved on February 24, 2019.

[15] K. Masch, "Über Elektronenionisierung von Stickstoff, Sauerstoff und Luft bei geringen und hohen Drucken", *Electrical Engineering (Archiv fur Elektrotechnik)*, vol.26, no. 8, pp.587-596, 1932.

[16] F. H. Sanders, "Measurement of the Townsend coefficients for ionization by collision", *Phys. Rev.*, vol. 44, no. 12, pp.1020-1024, 1933.

[17] [online] Available: Dutton database, www.lxcat.net, retrieved on February 24, 2019.

[18] A. A. Kulikovsky, "Positive Streamer between Parallel Plate Electrodes in Atmospheric Pressure Air", *J. Phys. D: Appl. Phys*, vol. 30, no. 3, pp. 441–450, 1997.

[19] O. Eichwald, M. Yousfi, O. Ducasse, “Breakdown criteria in air: an overview supported by predictive simulations”, *11ème Conférence de la Société Française d’Electrostatique,* Grenoble, France, 2018.
[20] V. Nikonov, R. Bartnikas, M. R. Wertheimer, "Surface charge and photoionization effects in short air gaps undergoing discharges at atmospheric pressure", *J. Phys. D: Appl. Phys*, vol. 34, pp. 2979-2986, 2001.
[21] B. Bagheri, J. Teunissen, U. Ebert, M.M. Becker, S. Chen, O. Ducasse, O. Eichwald, D. Loffhagen, A. Luque, D. Mihailova, J.M. Plewa, “Comparison of six simulation codes for positive streamers in air”, *Plasma Sources Sci. Technol.*, vol. 27, no. 9, pp. 095002, 2018.
[22] J. J. Lowke, F. D'Alessandro, "Onset corona fields and electrical breakdown criteria", *J. Phys. D: Appl. Phys.*, vol. 36, pp. 2673-2682, 2003.
[23] W. E. Bowls, "The effect of cathode material on the second Townsend Coefficient for ionization by collision in pure and contaminated nitrogen gas", *Phys. Rev.*, vol. 53, pp. 293-301, 1938.
[24] [online] Available: UNAM database, www.lxcat.net, retrieved on March 28, 2019
[25] S. K. Dahli, D. F. Williams, "Two-dimensional studies of streamers in gases", *J. Appl. Phys.*, vol. 62, pp. 4696-4707, 1987.
[26] P. Haefliger, and C.M. Franck, “Detailed precision and accuracy analysis of swarm parameters from a pulsed Townsend experiment”, *Rev. Sci. Instr.*, vol. 89, no. 2, pp.023114, 2018.
[27] Y. P. Raizer, “Gas Discharge Physics”, Germany, Berlin: Springer-Verlag, 1991.
[28] W. Wang, A. Bogaerts, " Effective ionisation coefficients and critical breakdown electric field of CO_2 at elevated temperature: Effect of excited states and ion kinetics ", *Plasma Sources Sci. Technol.*, vol. 25, no. 5, pp. 055025, 2016.
[29] D.K. Davies, “Ionization and attachment coefficients in CO_2: N_2: He and pure CO_2”, *J. Appl. Phys.*, vol. 49, no. 1, pp.127-131, 1978.
[30] R. Morrow, "A Survey of the Electron and Ion Transport Properties of SF_6", *IEEE Trans. Plasma Sci.*, vol. 14, no. 3, pp. 234-239, 1986.
[31] J. L. Hernandez-Avilla, J. de Urquijo, "Pulsed Townsend measurement of electron transport and ionization in SF_6–N_2 mixtures", *J. Phys. D: Appl. Phys.*, vol. 36, no. 12, pp. L51-L54, 2003.
[32] L. G. Christophorou, J. K. Olthoff, "Electron Interaction with SF_6", *J. Phys. Chem. Ref. Data*, vol. 29, no. 3, pp. 267-330, 2000.
[33] K. Satoh, H. Itoh, Y. Nakao, H. Tagashira, "Electron Swarm Development in SF_6. II. Monte Carlo Simulation", *J. Phys. D: Appl. Phys.*, vol. 21, pp. 931-936, 1988.
[34] H. Itoh, M. Shimozuma, H. Tagashira, S. Sakamoto, "Measurement of the Effective Ionization Coefficient and the Static Breakdown Voltage of SF_6 and Nitrogen Mixtures", *J. Phys. D: Appl. Phys.*, vol. 12, pp. 2167-2172, 1979.
[35] T. Aschwanden, "Swarm Parameters in SF_6/N_2 Mixtures Determined from a Time Resolved Discharge Study", *Proc. 4th Symp. on Gaseous Dielectrics (Knoxville, TN)*, pp. 24-32, 1984.
[36] H. Itoh, Y. Miura, N. Ikuta, Y. Nakao, H. Tagashira, "Electron Swarm Development in SF_6: I. Boltzmann Equation Analysis", *J. Appl. Phys.*, vol. 21, pp. 922-930, 1988.
[37] L. E. Kline, D. K. Davies, C. L. Chen, P. J. Chantry, "Dielectric Properties for SF_6 and SF_6 Mixtures Predicted from Basic Data", *J. Appl. Phys.*, vol. 50, no. 11, pp. 6789-6796, 1979.
[38] O. Ducasse, L. Papageorghiou, O. Eichwald, N. Spyrou, M. Yousfi, "Critical Analysis on Two-Dimensional Point-to-Plane Streamer Simulations Using the Finite Element and Finite Volume Methods," *IEEE Trans. Plasma Sci.*, vol. 35, no. 5, pp. 1287-1300, 2007.
[39] J. J. Lowke, F. D'Alessandro, "Onset corona fields and electrical breakdown criteria", *J. Phys. D: Appl. Phys.*, vol. 36, pp. 2673-2682, 2003.
[40] T. N. Tran, I. O. Golosnoy, P. L. Lewin, G. E. Georghiou, "Numerical modelling of negative discharges in air with experimental validation", *J. Phys. D: Appl. Phys.*, vol. 44, no. 1, pp. 015203, 2011.
[41] A. Bourdon, Z. Bonaventura, S. Celestin, "Influence of the pre-ionization background and simulation of the optical emission of a streamer discharge in preheated air at atmospheric pressure between two point electrodes", *Plasma Sour. Sci. Technol.*, vol. 19, no. 3, pp. 034012, 2010.
[42] D. K. Gupta, S. Mahajan, P. I. John, "Theory of step on the leading edge of negative corona current pulse", *J. Phys. D: Appl. Phys.*, vol. 33, no. 6, pp. 681-691, 2000.
[43] Y. V. Yurgelenas, H.-E. Wagner, "A computational model of a barrier discharge in air at atmospheric pressure: the role of residual surface charges in microdischarge formation", *J. Phys. D: Appl. Phys.*, vol. 39, no. 18, pp. 4031-4043, 2006.
[44] T. N. Tran, “Surface discharge dynamics: theory, experiment and simulation”, PhD Thesis, University of Southampton, 2010.
[45] X. Chen, W. He, X. Du, X. Yuan, L. Lan, X. Wen, B. Wan, “Electron swarm parameters and Townsend coefficients of atmospheric corona discharge plasmas by considering humidity”, *Phys. Plasmas*, vol. 25, no. 6, pp. 063525, 2018.
[46] H. Hasegawa, H. Date, M. Shimozuma, K. Yoshida, H. Tagashira, "The Drift Velosity and Longitudinal Diffusion Coefficient of Electrons in Nitrogen and Carbon Dioxide from 20 to 1000 Td", *J. Phys. D: Appl. Phys.*, vol. 29, pp. 2664-2667, 1996.
[47] H. Schlumbohm, “Messung der Driftgeschwindigkeiten von Elektronen und positiven Ionen in Gasen”, *Zeitschrift für Physik*, vol. 182, no. 3, pp.317-327, 1965.
[48] T. Huiskamp, A. J. M. Pemen, W. F. L. M. Hoeben, F. J. C. M. Beckers, E. J. M. van Heesch, "Temperature and pressure effects on positive streamers in air", *J. Phys. D: Appl. Phys.*, vol. 46, no. 16, pp. 165202-165210, 2013.
[49] S. V. Pancheshnyi, A. Y. Starikovskii, "Two-dimensional numerical modeling of the cathode-directed streamer development in a long gap at high voltage", *J. Phys. D: Appl. Phys.*, vol. 36, no. 21, pp. 2683-2691, 2003.
[50] Y.V. Serdyuk, A. Larsson, S.M. Gubanski, M. Akyuz, "The propagation of positive streamers in a weak and uniform background electric field", *J. Phys. D: Appl. Phys.*, vol. 34, no. 4, pp. 614-623, 2001.
[51] F. Shi, N. Liu, H. K. Rassoul. "Properties of relatively long streamers initiated from an isolated hydrometeor", *J. Geophys. Res: Atmos., vol.* 121, no. 12, pp.7284-7295, 2016.
[52] M. Seeger, J. Avaheden, S. Pancheshnyi, T. Votteler, "Streamer parameters and breakdown in CO_2", *J. Phys. D: Appl. Phys.*, vol.50, pp.015207, 2017.
[53] J. Won, P. F. Williams, "Experimental study of streamers in pure N_2 and N_2/O_2 mixtures and a ≈13 cm gap", *J. Phys. D: Appl. Phys.*, vol. 35, no. 3, pp. 205-218, 2002.
[54] E. M. van Veldhuizen, W. R. Rutgers, "Inception behaviour of pulsed positive corona in several gases", *J. Phys. D: Appl. Phys.*, vol. 36, no. 21, pp. 2692-2696, 2003.
[55] L. Gould, L. W. Roberts, "Breakdown of air at microwave frequencies", *J. Appl. Phys.*, vol. 27, no. 10, pp. 1162-1170, 1956.
[56] W.S. Kang, J.M. Park, Y. Kim, S.H. Hong, "Numerical study on influences of barrier arrangements on dielectric barrier discharge characteristics", *IEEE Trans. Plasma Sci.*, vol. 31, no. 4, pp. 504-510, 2003.
[57] X. Chen, L. Lan, H. Lu, Y. Wang, X. Wen, X. Du, W. He, “Numerical simulation of Trichel pulses of negative DC corona discharge based on a plasma chemical model”, *J. Phys. D: Appl. Phys.*, vol. 50, no. 39, pp.395202, 2017.
[58] A. Hallac, G. E. Georghiou, A. C. Metaxas, "Secondary emission effects on streamer branching in transient non-uniform short-gap discharges", *J. Phys. D Appl. Phys.*, vol. 36, no. 20, pp. 2498-2509, 2003.
[59] P. A. Vitello, B. M. Penetrante, J. N. Bardsley, "Simulation of negative streamer dynamics in nitrogen", *Phys. Rev. E,* vol. 49, no. 6, pp. 5574-5598, 1994.
[60] P.G. Davies, J. Dutton, F.L. Jones, “The motion of slow positive ions in gases-Mobilities of potassium and nitrogen ions in nitrogen”, *Philosophical Transactions of the Royal Society of London, Series A, Mathematical and Physical Sciences*, vol. 259, no. 1100, pp.321-330, 1966.
[61] E.W. McDaniel, and E.A. Mason, “Mobility and diffusion of ions in gases”. *Wiley, New York*, 1973.
[62] D. H. Douglas-Hamilton, "Recombination rate measurements in nitrogen", *J. Chem. Phys.*, vol. 58, no. 11, pp. 4820-4823, 1973.
[63] A. J. Davies, C. S. Davies, C. J. Evas, "Computer simulation of rapidly developing gaseous discharges", *Proc. Inst. Electr. Eng.*, vol. 118, no. 6, pp. 816-823, 1971.
[64] A. A. Kulikovsky, "The structure of streamers in N_2. II. Two-dimensional simulation", *J. Phys. D: Appl. Phys.*, vol. 27, pp. 2564-2569, 1994.
[65] H. Schlumbohm, “Stoßionisierungskoeffizient α, mittlere Elektronenenergien und die Beweglichkeit von Elektronen in Gasen”, *Zeitschrift für Physik*, vol. 184, no. 5, pp.492-505, 1965.
[66] L. A. Viehland, C. C. Kirkpatrick, "Relating ion/neutral reaction rate coefficients and cross-sections by accessing a data base for ion transport properties", *Int. J. Mass Spectrom. Ion Proc.*, vol. 149, pp. 555-571, 1995.

[67] S. Ponduri, "Understanding CO_2 containing non-equilibrium plasmas: modeling and experiments", *PhD Thesis*, *Technische Universiteit Eindhoven, Eindhoven*, 2016.
[68] H. Jungblut, D. Hansen and W. F. Schmidt, "Ion-ion recombination in electronegative gases," *IEEE Trans. Electr. Insul.*, vol. 24, no. 2, pp. 343-348, 1989.
[69] U. Ebert, S. Nijdam, C. Li, A. Luque, T. Briels, "Review of recent results on streamer discharges and discussion of their relevance for sprites and lightning", *Journal of Geophysical Research*, vol. 115, A00E43, 1-13, 2010.

Ting Liu was born in Wuhan, China. She received the M.Sc. degree in Control Science and Engineering from Wuhan University of Technology, China, in 2011. After her graduation, Ting joined Philips Lighting Luminaires (Shanghai) Co., Ltd. as an Engineer.
Currently she is pursuing her Ph.D. degree in High Voltage Technology at the Department of Electronic and Electrical Engineering, University of Strathclyde, Glasgow, U.K. Her current research interests include pulsed power, transient plasma and streamers, pulsed breakdown in gases.

Igor V. Timoshkin (M'07–SM'14) received the degree in physics from Moscow State University, Moscow, Russia, in 1992, and the Ph.D. degree from the Imperial College of Science, Technology and Medicine (ICSTM), London, U.K., in 2001.
He was a Researcher at Moscow State Agro-Engineering University, Moscow, and then at the Institute for High Temperatures of Russian Academy of Sciences, Moscow. In 1997 he joined ICSTM. Then he joined the Department of Electronic and Electrical Engineering, University of Strathclyde, Glasgow, U.K., in 2001, where he became a Reader in 2016. His research interests include dielectric materials, pulsed power, transient plasma discharges, environmental applications of non-thermal plasma discharges.
Dr. Timoshkin is a Voting Member of the Pulsed Power Science and Technology Committee in the IEEE Nuclear and Plasma Science Society; a member of International Advisory Committee of the IEEE Conference on Dielectric Liquids, a member of the International Scientific Committee of the Gas Discharges and Their Application Conference, and a Subject Editor of IET Nanodielectrics.

Scott J. MacGregor (M'95–SM'14) received the B.Sc. and Ph.D. degrees from the University of Strathclyde, Glasgow, U.K., in 1982 and 1986, respectively.
He was a Pulsed-Power Research Fellow in 1986 and a Lecturer in pulsed-power technology in 1989. In 1994, he became a Senior Lecturer, with a promotion to a Reader and a Professor of High Voltage Engineering, in 1999 and 2001, respectively. In 2006 and 2010, he became the Head of the Department of Electronic and Electrical Engineering and the Executive Dean of the Faculty of Engineering, and has been the Vice-Principal with the University of Strathclyde, since 2014. His current research interests include high-voltage pulse generation, high-frequency diagnostics, high-power repetitive switching, high-speed switching, electronic methods for food pasteurization and sterilization, the generation of high-power ultrasound (HPU), plasma channel drilling, pulsed-plasma cleaning of pipes, and the stimulation of oil wells with HPU. Prof. MacGregor was a recipient of the 2013 IEEE Peter Haas Award. He was an Associated Editor of the IEEE Transitions On Dielectrics and Electrical Insulation in 2015.

Mark P. Wilson (M'10) was born in Stranraer, Scotland, in 1982. He received the B.Eng. (with honours), M.Phil., and Ph.D. degrees in electronic and electrical engineering from the University of Strathclyde, Glasgow, U.K., in 2004, 2007, and 2011, respectively. He is presently based in the High Voltage Technologies research group at the University of Strathclyde, where his research interests include interfacial surface flashover, nanodielectrics, and the practical applications of high power ultrasound, corona discharges, and pulsed electric fields. Mark is a member of the IEEE Nuclear and Plasma Sciences Society, from whom he received a Graduate Scholarship Award in 2011, the IEEE Dielectrics and Electrical Insulation Society, and the IET.

Martin J. Given (M'99–SM'11) received the B.Sc. degree in physics from the University of Sussex, Brighton, U.K., in 1981, and the Ph.D. degree in electronic and electrical engineering from the University of Strathclyde, Glasgow, U.K., in 1996.
He is currently a Senior Lecturer with the Department of Electronic and Electrical Engineering, University of Strathclyde. His current research interests include aging processes and condition monitoring in solid and liquid insulation systems, high-speed switching, and pulse power.

Nelly Bonifaci graduated from University Joseph Fourier with a MEng degree in Physics in 1989. In 2008 she obtained the HDR Habilitation qualification from the University of J Fourier, Grenoble. Dr Bonifaci joined the Laboratory on Dielectric Materials and Electrostatics (now G2E laboratory) CNRS, France in 1989 where she became a 1st class researcher in 1997. In 2007 she was promoted to a position of a Senior Researcher/Team Leader. Dr Bonifaci research interests include breakdown in insulating liquids, plasma streamers in liquid dielectrics, pre-breakdown and plasma phenomena in dielectric liquids including corona discharges and electronic transport. Dr Bonifaci is an Editor of the IEEE Transactions of Dielectric and Electrical Insulation and a member of International Advisory Committee of the IEEE Conference on Dielectric Liquids.

Rachelle Hanna received her PhD in Electrical Engineering from the University of Toulouse in 2012. She is presently Associate Professor at Grenoble Institute of Technology. Her main research topics are the electrical characterization and modelling of dielectric materials under ionizing radiation, high temperature and very high voltage.